

## Field Test Study on a Short Pile-net Composite Foundation over Gravel Clay for High-Speed Railways

Yong-hui Shang<sup>1,2\*</sup>, Lin-rong Xu<sup>1</sup>, Yan-qun Xu<sup>1</sup>, Yi-jie Li<sup>1</sup> and Ning-yi OU<sup>3</sup>

<sup>1</sup>School of Civil Engineering, Central South University, Changsha 410083, China

<sup>2</sup>Institute of Architecture and Engineering, Huang Huai University, Zhumadian 463000, China

<sup>3</sup>Center of International Affairs, CEKII Civil Engineering Co .Ltd., Kowloon, Hong Kong

Received 1 April 2016; Accepted 30 June 2016

### Abstract

To solve the key issues of stress transfer law and settlement mechanism in a pile-net composite foundation, the geosynthetic-reinforced and short pile-supported embankment over gravel clay with low to moderate compressibility at the DK86+998.0-DK87+191.2 section of the Ganzhou-Longyan High-speed Railway was selected as a case study. Field tests that combine theoretical analysis with analytic calculation were conducted to investigate the change laws of stress acting on the pile and the subsoil, pore water pressure, and foundation deformation, as well to predict pile-net composite foundation settlement. Results show that the stress distribution exhibits a saw-toothed shape across the foundation, and the reaction force of the foundation varies against the filling embankment load. After constructing the embankment, the average pile-soil stress ratio is 4.0 and the pile-soil load ratio reaches 50%. Foundation deformation mainly appears during the construction phase with an accumulative ground settlement of 55 mm and an accumulative lateral displacement of 25 mm. Unlike that of in-situ measurement, the accumulative settlement of the foundation is predicted to be 62 mm in a 2000-day duration, whereas the accumulative settlement increases only by 7 mm following the 800-day predictive period. Result also indicates that soil consolidation mainly occurs during the construction period and the effect of the engineering control of using short piles for the foundation is evidently effective. This approach is low-cost and convenient to construct. Prior selection of short piles for foundation enforcement is suggested for cases under similar geological conditions.

*Keywords:* Pile-net Composite Foundation, Stress Transfer, Settlement Mechanism, Field Test

### 1. Introduction

The pile-net composite foundation was first used in the embankment reconstruction project of Ishikari in Hokkaido, Japan in 1975 [1]. In 1994, it was applied for the first time in China in the Nanning-Kunming Railway line [2]. With technical improvement, the pile-net composite foundation has been extensively applied in reinforcing the soft soil foundation of high-speed railways [3]. The pile-net composite foundation mainly consists of six parts [4]: the upper embankment fill, the grid network, the sand-gravel cushion, the reinforced area in the pile-soil composite region, the pile-soil underlying soft soil layer, and the bearing layer. Unlike in single composite foundations [5], the net and the soil work together to share the upper load in pile-net composite foundations [6]. This composite foundation type combines horizontal and vertical reinforcement. Pile-net composite foundations can be divided according to foundation type into flexible pile-net, semi-rigid pile-net, and granular pile-net composite foundations [7], [8].

Pile-net composite foundations are used locally and abroad and are known as pile-supported reinforced embankments [9], pile-net structure supported embankments

[10], and pile-net structure foundation [11]. Although these terms vary, they are all categorized as pile-net composite foundations in terms of their reinforcement mechanism. Local and foreign studies on the reinforcement effect of pile-net composite foundations have discussed the construction and operation periods of such foundations from the perspective of time and the embankment-composite foundation structure system from the perspective of space. Various theories have been developed in these studies, including the membrane effect [12] and the soil arching effect [13]. Research methods include theoretical calculation [8], numerical simulation [11], field test [12], and laboratory experiment [14]. Theoretical research is based on many assumptions. Thus, determining the actual situation of deformation of a rigid pile composite foundation under stress is difficult. Numerical simulations can consider pile-soil coupling stress. However, selecting the constitutive relations and boundary conditions of a model is complicated. Laboratory model tests can be used to analyze multiple conditions, which is important in engineering applications. However, identifying the wireless domain of a foundation is difficult. A field test is the most commonly used method in this area. For example, Gong [15] discussed the behavior of a composite foundation under a flexible foundation and pointed out that the working mechanism of the composite foundation cushion differed under flexible and rigid foundations. Xu et al. [16] studied basement soil pressure, geogrid strain, and ground settlement during the construction

\* E-mail address: mlpeter@163.com

of a pile-net composite foundation by conducting a field test on the pile-net composite foundation at the Kunshan test section in the Beijing-Shanghai High-speed Railway.

Other countries have improved the design and construction specifications of pile-net composite foundations because of the increasing applications of this type of foundation. However, many problems still have to be addressed, such as its bearing mechanism and deformation law. China has a wide distribution of medium compressible soil (compaction coefficient: 0.1 to 0.5). Thus, examining various treatments for similar engineering practices is significant. The load transmission law and deformation characteristics at the top of a foundation are studied. The foundation reinforcement control effect is evaluated for nearly 400 days based on actual measured data of gravel clay (compaction coefficient: 0.2 to 0.3, low to moderate compressible soil) in the short pile-net composite foundation at the DK86+998.0-DK87+191.2 test section of the Ganzhou-Longyan High-speed Railway to provide a reference for similar engineering practices.

## 2. Working Mechanism of Pile-net Composite Foundation

The load transmission mechanism of the pile-net composite foundation in this collaborative work is shown in Fig. 1. In this figure,  $B$  is the width of the soil between piles,  $H$  is the height of the embankment,  $q_0$  is the uniform load of the embankment,  $W_1$  is the weight of the soil between piles,  $W_2$  is the weight of the pile top soil,  $\tau$  is the shear stress along the soil wedge,  $\sigma_s$  is the stress acting on the foundation soil,  $\sigma_c$  is the stress acting on the pile, and  $T$  is the tension of the geogrid material.

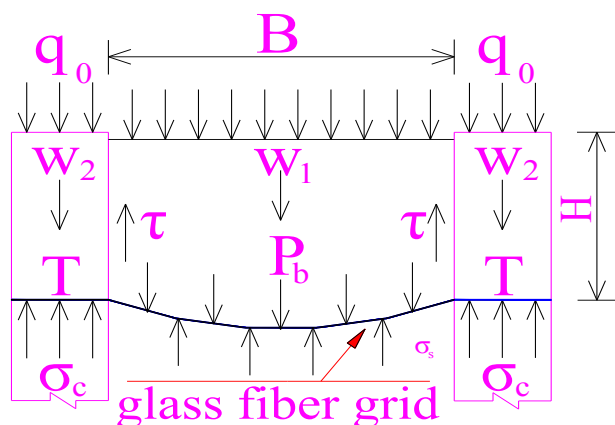


Fig.1. Load transmission mechanism of the pile-net composite foundation

(1) Soil arching effect. The rigidity of the soil between piles varies. Under the action of self-weight ( $W_1$ ) of soil between piles, the settlements of the pile top soil and the soil between piles differ. The settlement of the latter is greater than that of the former. The direction of the major principal stress is deflected because of the stress redistribution caused by the change in soil displacement, which leads to soil compaction in the arched area of the adjacent piles and the formation of compacted crust arch with high rigidity. The compacted crust arch redistributes the upper load to the pile top. This phenomenon is called the soil arching effect.

(2) Membrane effect. In the replacement layer of the tensile reinforcement, the interface stress transmission of the soil and the geosynthetics (e.g., geogrid and geotextile) changes the original stress distribution of the soil. When the geosynthetics have only one layer, the reinforced cushion acts like a tension membrane. This phenomenon is called the membrane effect.

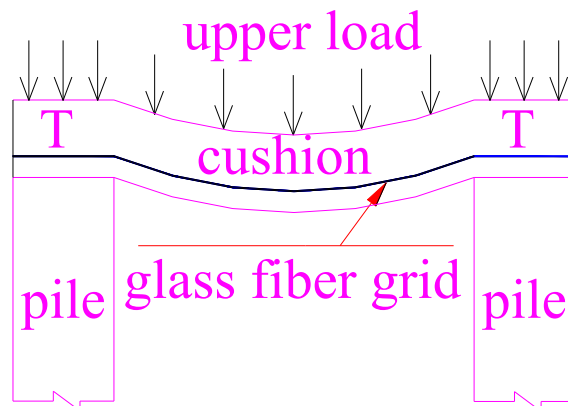


Fig.2. Membrane effect

(3) Bridging effect. When multiple layers of geosynthetics are laid over the composite foundation or only a few layers are used, the rigidity satisfies certain conditions because of the occlusion and friction between the geosynthetics and the soil. The reinforced cushion acts like a beam or a plate, which limits the lateral displacement on the surface of the foundation, results in the uniform distribution of the vertical load, and significantly reduces the differential settlement of the pile and the soil. This phenomenon is called the bridging effect.

The results described above typically occur simultaneously because of the settlement difference of soil between piles, which is caused by the rigidity difference between the piles. The load transmission process under the action of the reinforced geosynthetics cushion is indicated by the pile-soil stress ratio (Equation (1)):

$$n = \sigma_c / \sigma_s \quad (1)$$

where  $n$  is the pile-soil stress ratio;  $\sigma_c$  is the pile top stress; and  $\sigma_s$  is the stress between piles. Pile-net composite foundations are frequently arranged in a square. This study derives the pile-soil stress ratio based on this type. Pile spacing is  $d$ , and the pile diameter is  $R$ . Thus, force  $F_1$  produced by the pile top stress  $\sigma_c$  to support a soil column on the upper part is:

$$F_1 = 0.25\pi R^2 \sigma_c \quad (2)$$

Force  $F_2$  created by the stress  $\sigma_s$  of the soil between piles to support a soil column on the upper part is:

$$F_2 = \sigma_s d^2 \quad (3)$$

The angle between tension  $T$  is assumed to be produced because of the grid membrane effect, and the horizontal direction is  $\varphi$ . The following equations can be obtained based on the mechanical equilibrium condition:

$$Hd^2\gamma = F_1 + F_2 + 2T \sin \varphi \tag{4}$$

$$T = \varepsilon Ed \tag{5}$$

where  $\gamma$  is the volume weight of the embankment fill;  $\varepsilon$  is the grid strain under normal working conditions; and  $E$  is the tensile modulus of the grid (kN/m) measured by the test.

The post-construction settlement of the embankment is set as  $U$ . The shape of the settlement caused by the membrane effect is approximately regarded as a parabola that passes  $(0.5d, U)$ . Thus, the parabolic equation is

$$F(x) = 4Ud^{-2}x^2 \tag{6}$$

The following can be obtained from Equation (6):

$$\sin \varphi = 4U(16U^2 + d^2)^{-1} \tag{7}$$

The value of  $\sigma_s$  is assumed to exhibit the following relationship with the standard bearing capacity  $F_f$  of soil between piles:

$$\sigma_s = mF_f \tag{8}$$

The pile-soil stress ratio  $n$  can be expressed as follows according to preceding equations:

$$n = \frac{Hd^2\gamma - d^2mF_f - 8Ud\varepsilon E(16U^2 + d^2)^{-1}}{0.25\pi R^2\sigma_s mF_f} \tag{9}$$

### 3 Engineering Situation of the Test Section and the Test Scheme

#### 3.1 Engineering Situation

The Ganzhou-Longyan High-speed Railway is 290.1 km long. Its construction started in 2010, and it is expected to be open to traffic in 2016. The design speed is equal to or greater than 50 km/h. The test section is located near Xiaomi Town in Du County, Ganzhou City with a design mileage of DK86+998.0–DK87+191.2. The total length of the railway is 192.88 m (including 0.32 m short chains). It is located in a piedmont gentle slope with a flat topography. The track in the test section is ballastless.

The foundation strata (from top to bottom) in the test section are as follows: (1) silty clay ( $Q^{4al+pl}$ ): ochre to tan; hard plastic; mainly clayey soil; uniform soil; smooth cutting surface; local gravel content: 2% to 5%; particle size: 2 nm to 10 mm, mostly sand and fine round gravel; layer depth: 0.5 m to 15 m; bearing capacity: 160 kPa. (2) silty clay ( $Q^{el+dl}$ ): tan; hard plastic; mainly clayey soil; uniform soil; contains Fe-Mn nodules; rough cutting surface; local rougher cut; local gravel content: 5% to 30%; particle size: 2 mm to 20 mm, 60 mm for individuals, mostly sandstone weathering fragments, angular and gravelly; layer depth: 8 m to 25 m; bearing capacity: 180 kPa. (3) limestone ( $C_2h$ ): blue gray; weak weathering; karst development; bearing capacity: 800 kPa. The specific physical and mechanical parameters of the layers are provided in Table 1.

The groundwater in the test section is mainly composed of carbonate paleokarst water, followed by quaternary pore water. The buried depth of quaternary pore water is 1.5m to 12.7m, which is easily affected by seasonal variation. Groundwater and surface water in the entire test section are not aggressive.

**Table 1.** Physical and mechanical parameters of the soil layer (average value)

Foundation Soil Layer I	Natural Water Content (%)	Natural Density (g/cm <sup>3</sup> )	Natural Void Ratio	Liquid Limit (%)	Plastic Limit (%)	Internal Friction AngleΦu(°)	Cohesion Cu(kPa)	Compressibility	Compression Modulus(MPa)
Q <sub>4</sub> <sup>al+pl</sup> Silty clay	24.18	1.95	0.75	41.32	21.27	21.85	57.12	0.24	7.42
Q <sup>el+dl</sup> Silty clay	24.03	2.00	0.70	37.91	19.33	15.94	49.88	0.24	7.19

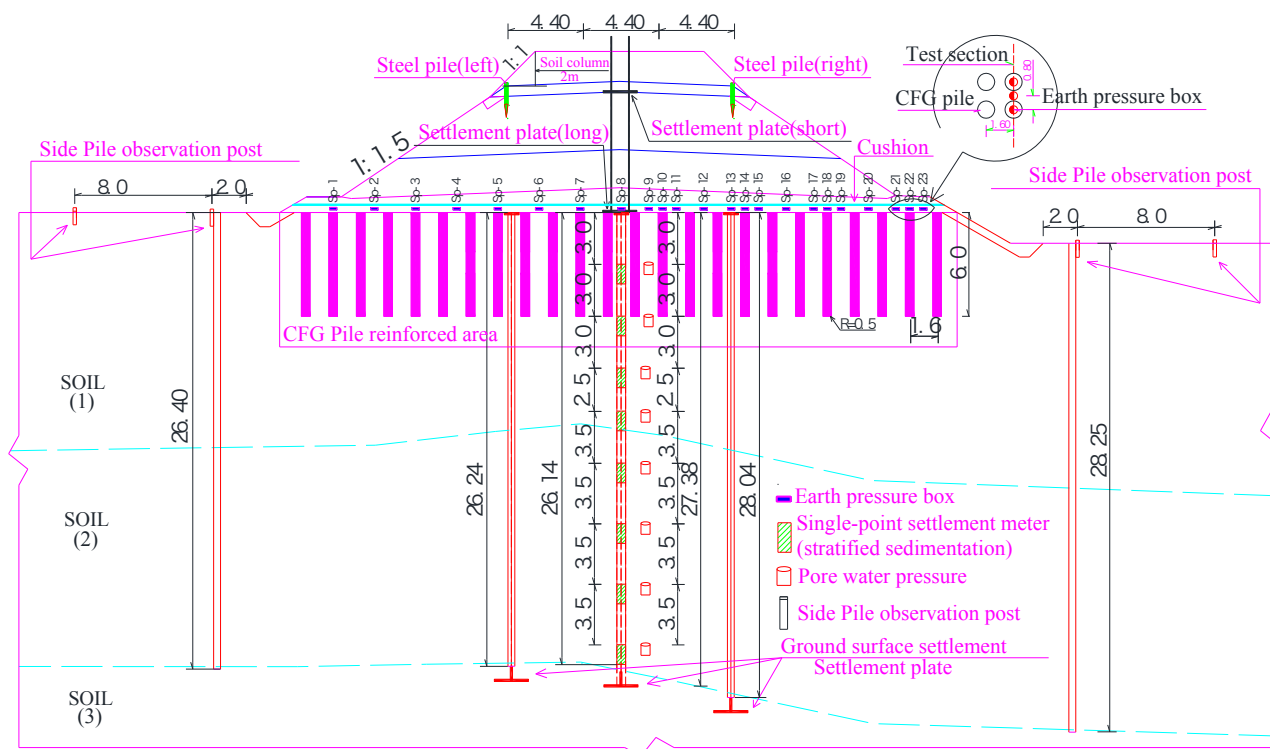


Fig. 3. Test Component Layout (DK87+185.000 Section)

Table 1 shows that gravel clay is characterized by low water content, low void ratio, high liquid limit, overconsolidation, and low moderate compressibility. The natural foundation exhibits a low bearing capacity. It adopts the cement-flyash-gravel (CFG) pile + geogrid + gravel cushion measure for treatment. CFG piles are arranged in a square with a spacing of 1.6 m, a diameter of 0.5 m, and a length of 6 m. A layer of TGDG100KN/m one-way overall polypropylene tensile geogrid is laid on the pile top cushion (0.4 m deep gravel cushion + 0.2 m deep medium coarse sand) with an elongation of 10% or less. The embankment filling is 7.1 m high with a top width of 13.2 m and a slope of 1:1.5.

**3.2 Test Scheme**

**Test project:** Ground settlement, foundation layered settlement, lateral displacement of the foundation, soil pressure between the pile top and the soil between piles, geogrid displacement, and pore water pressure.

**Data collection:** The settlement plate was buried in the surface. DL-502 type electronic level was used to measure the settlement with a measurement accuracy of 0.4 mm. PVC pipes and a YH-2620A-type single-point extensometer series-connected system were buried under the surface of the foundation center. A YH6406 digital reader was used to test ground settlement. Side piles were buried on both sides of the section. An XB338-2 type sliding inclinometer was used to test the lateral displacement of the foundation. A JMZX-5020AT-type intelligent string earth pressure cell was buried at the pile top and the soil between piles with a sensitivity of 0.001 MPa. A JMZX-3001-type integrated test instrument was used to collect data. A JMDL-2405A-type flexible displacement gauge was utilized to measure geogrid displacement with a sensitivity of 0.001 mm. A JMZX-5503AT-type pore pressure gauge was used to measure pore water pressure with a sensitivity of 0.001 MPa. The specific layout of the test components is shown in Fig. 3, and the field component embedment layout is presented in Fig. 4.



Fig. 4. Instrument embedment construction site photos

Burying time of test components: November 6, 2012; starting time of the test: January 26, 2013; ending time of the test: January 6, 2015; test frequency in the foundation filling stage: once a day; settlement mutation time: two to three times per day; test frequency in the foundation standing period after end of filling: twice a week during the first to third months and once a month after three months.

**4 Test Results and Analysis**

**4.1 Soil Pressure Test Result Analysis**

**4.1.1 Soil pressure -Time- Filling Height Change Curve**

To facilitate expression, the foundation filling is divided into four periods based on time, as shown in Table 2.

Table 2. Filling stage division

Phase Division	Time interval	Accumulative Filling Height (m)
----------------	---------------	---------------------------------

Early Phase of Filling	2013/10/27~2014/01/09	2.7
Medium Phase of Filling	2014/01/09~2014/04/15	2.7
Later Phase of Filling	2014/04/15~2014/05/27	7.1
Dead Load Phase	2014/05/27~2015/01/06	7.1

Fig. 5 presents the change curves of the soil pressures at the pile top and between piles with time and filling height. The figure indicates that the change laws of soil pressure at the pile top and between piles with time and filling height are similar. The soil pressure at the pile top is greater than that between piles because of the objective rigidity difference of soil between piles. During the initial stage of the early phase of filling, low accumulative soil pressure is mainly attributed to low filling load, and the wide fluctuation of the curve is caused by large filling construction machinery. During the medium phase of filling, the soil pressure curve tends to develop linearly because the filling height remains. During the later phase of filling, the upper load increases and soil pressure begins to increase with filling height. During the dead load period, soil pressure tends to develop linearly mainly because the net, cushion, and soil between piles are coordinated. The foundation tends to stabilize after stress is balanced.

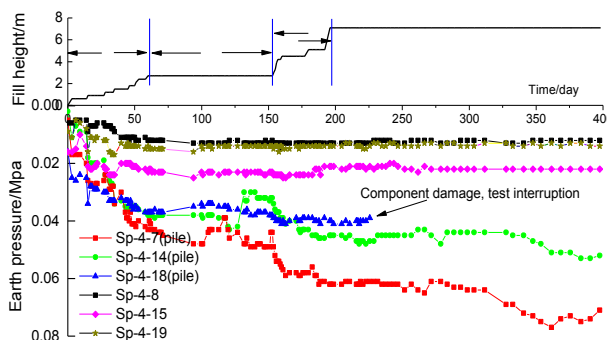


Fig. 5. Soil pressure-time-filling height change curve

The accumulative soil pressure values of different test points during various phases and their proportions are presented in Table 3. Sp-4-18 (Pile) is excluded because of the lack of data. Table 3 indicates that the soil pressure during the early phase of filling accounts for a large proportion, during which the soil pressure at the pile top accounts for over 60% and that between piles reaches over 90%. These results demonstrate that the pile-net composite foundation structures exhibit the most frequent coordination and stress dynamic balance in this phase from the side. Under this condition, the soil arching effect and the membrane effect of the grid occur. The upper embankment fill load is effectively transmitted to the lower foundation structure.

Table 3. Accumulative soil pressures of different test points at different phases and their proportions

Test point	Distance from One Side of the Foundation Center	Early Phase of Filling		Medium Phase of Filling		Later Phase of Filling		Dead Load Phase	
		Accumulative Value	Proportion	Accumulative Value	Proportion	Accumulative Value	Proportion	Accumulative Value	Proportion
SP-4-7(Pile)	0m	0.034Mpa	65.38%	0.035Mpa	1.92%	0.045Mpa	19.23%	0.052Mpa	13.46%
SP-4-14(Pile)	9.6m(Right)	0.054Mpa	76.06%	0.055Mpa	1.41%	0.062Mpa	9.86%	0.071Mpa	12.67%
SP-4-8(Soil)	2.4m(Right)	0.013Mpa	92.86%	0.013Mpa	0.00%	0.014Mpa	7.15%	0.014Mpa	0.00%
SP-4-15(Soil)	10.4m(Right)	0.021Mpa	91.30%	0.022Mpa	4.35%	0.023Mpa	4.35%	0.023Mpa	0.00%
SP-4-19(Soil)	15.2m(Right)	0.014Mpa	93.33%	0.014Mpa	0.00%	0.015Mpa	6.67%	0.015Mpa	0.00%

#### 4.1.2 Lateral Distribution Law of Soil Pressure Along the Foundation

Fig. 6 indicates the changing curve of the lateral distribution of soil pressures along the foundation. The figure shows that the soil pressures are distributed laterally in a saw-toothed shape along the foundation. The pressure at the pile top is greater than that between piles. Soil pressures at the pile top and between piles are inversely proportional to the distance of the piles to the foundation center. The soil pressure at the top of SP-4-10 (Pile) on the right side of the foundation is evidently greater than those at the other test points mainly because a deformation lane is set above the test point and soil pressure is affected by traffic load.

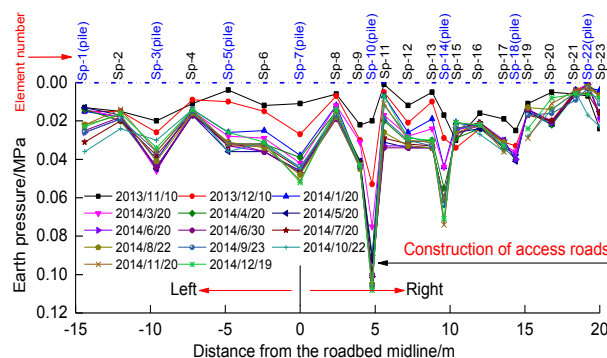


Fig. 6. Lateral distribution change curves of soil pressure along the foundation

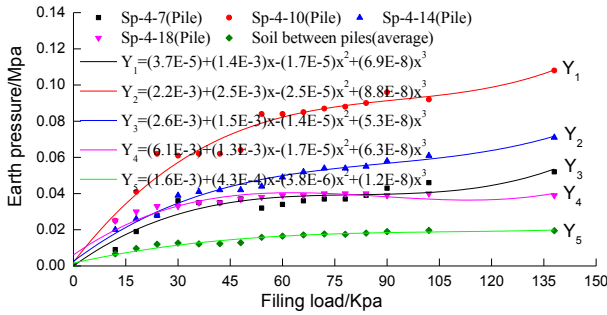


Fig.7. Soil pressure change fitting curves along the load

To further explore the foundation reaction characteristics of the gravel clay short pile-net composite foundation of the test section and to provide important parameters for engineering applications, the actual measured values of soil pressures at different test points of the foundation are adopted for curve fitting. The results are shown in Fig. 7. The figure indicates that both the curve changes of soil pressure at the pile top and the average soil pressure of soil between piles along with the filling load follows the cubic polynomial function. The fitting curves highly coincide with the actual measured values. Thus, the curves can reflect the internal law of the change of the foundation reaction with load.

**4.1.3 Change Law of the Pile-soil Stress (Load Sharing) Ratio**

Pile-stress ratio is an important parameter of the composite foundation that is difficult to determine accurately [12]. Many local and foreign scholars have directly tested pile-soil stress through static load tests by laying the pressure cell at the top of the pile and soil; these scholars have obtained the pile-soil stress ratio according to its definition to perform test analysis and research [12].

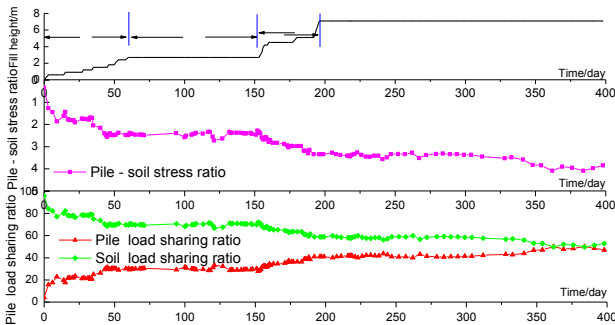


Fig. 8. Pile-soil stress (load) ratio-time-filling height change curves

Fig. 8 shows that the pile-soil stress ratio increases gradually with filling height. This result occurs mainly because the concentration degree of the pile stress gradually increases as a result of the pile-soil difference settlement. After the dead load phase, the accumulative pile-soil stress ratio is approximately 4, which indicates that the pile can effectively bear the load. The pile-soil load sharing ratio is approximately 50%, which indicates that the geogrid-reinforced cushion plays a crucial adjusting role. Thus, the soil between piles exhibits better bearing capability.

**4.2 Grid Strain Test Result Analysis**

Fig. 9 shows the grid displacement change curve with time and filling height. The figure indicates that during the beginning of filling, geogrid strain increases rapidly and decreases to a stable stage because it is affected by vehicle

load during construction. When filling height slightly increases, the strain tends to change in a straight line. As shown in the grid strain curve, the geogrid strain at the top of the pile is greater than that at the soil between piles. This outcome mainly occurs because the pile top with high rigidity has a constraint function on the grid. However, the rigidity of the soil between piles is low. The settlement forces the geogrid to receive the force in a net bag shape, which leads to a high strain.

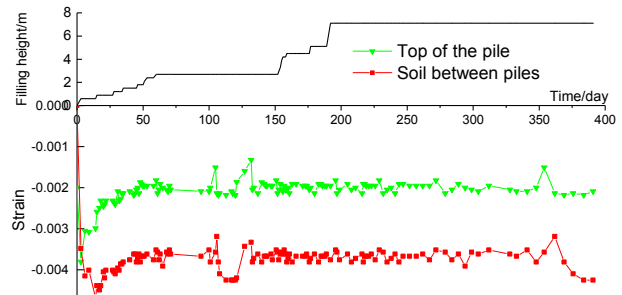


Fig.9. Geogrid strain-time-filling height change curves

During the final stable phase, the geogrid strain at the top of the pile is 0.002 and the geogrid strain between piles is 0.004. These values are relatively small with a large gap from the designed breaking elongation rate of 10%. This result indicates that the geogrid strain is far from reaching the designed tensile strength of 100 KN/m, and it has not been fully used, which is related to the short pile spacing. In future engineering applications, similar approaches can optimize the pile spacing or reduce the intensity of geogrids and satisfy the requirements for foundation stability and deformation for an economical project construction.

**4.3 Analysis of the Underground Pore Water Pressure Test Results**

Fig.10 shows the change curves of underground pore water pressures with the time and filling height.

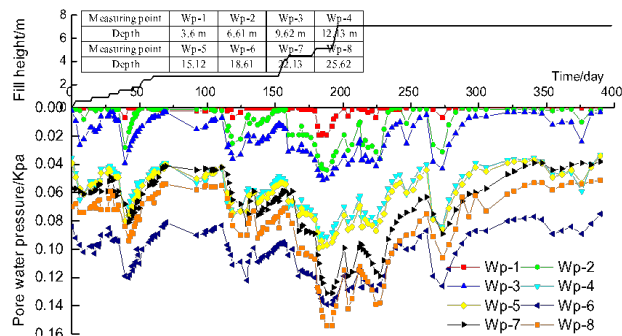


Fig.10. Pore water pressure-time-filling height change curves

Fig. 10 indicates that the pore water pressure changes in a wavy shape mainly because the filling load in this phase is relatively low. During the later phase of filling, the pore water pressure fluctuates significantly because under the consolidation effect of soil, the underground stress field is balanced repeatedly. Pore water pressures at the test points in the short pile-reinforced area change slightly. However, those at the end of the piles change significantly. This result occurs because under the influence of the soil arching effect and the membrane effect of the geogrid, the additional stress produced by the filling load at the top of the foundation can

be transmitted from the piles to the soil layer at the end of the piles, which increases the additional stress of the soil layer at the end of the piles. Thus, pore water pressure significantly changes. This outcome also verifies that short piles can effectively transmit an additional stress increment of the upper load to the side.

#### 4.4 Analysis of the Foundation Deformation Test Results

##### 4.4.1 Foundation Settlement-Time-Filling Height Change Curve

The monitoring data of surface settlement in Fig. 11 show that accumulative settlement increases gradually with filling load. During the beginning of filling, the settlement rate reaches as high as 0.63 mm/d and the accumulative settlement value reaches 38 mm, which accounts for 69.09% of the total value. During the middle phase of filling, the filling height remains the same and the settlement still develops slowly mainly because soil consolidation is affected by time. During the later phase of filling, the settlement continues to develop with a settlement rate of only 0.11 mm/d, and the accumulative settlement value is 52 mm when filling height increases. During the dead load phase, soil consolidation is completed. Thus, the settlement curve changes slowly and develops linearly with the final accumulative settlement value of 55 mm.

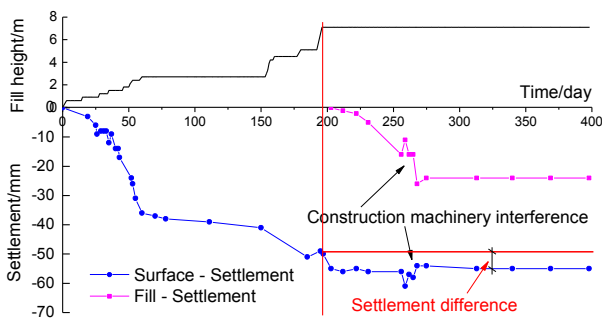


Fig.11. Surface (embankment) settlement-time-filling height change curves

The compaction situation of the foundation filling soil is crucial in post-construction settlement control. Embankment deformation is appropriately defined as the difference between the actual settlement value of the short settlement plate and the accumulative surface settlement value. Fig. 11 shows that the foundation fill settlement is mainly concentrated 50 days before the preloading period with a settlement rate of 0.44 mm/d and an accumulative settlement of 22 mm. Then, 50 days after preloading, the settlement change is approximately 0, which verifies the good compaction control effect of the embankment fill from the side.

##### 4.4.2 Ground Settlement-Time-Filling Height Change Curve

Fig. 12 presents the change curves of ground settlement with time and filling height. The buried depths of test points MS-1, MS-2, MS-4, MS-5, and MS-7 are 3, 6, 11.5, 14.5, and 21.5 m, respectively.

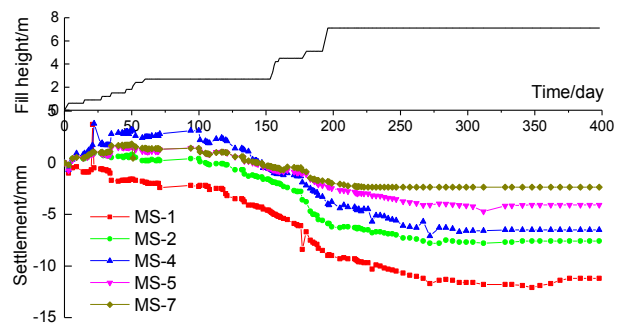


Fig.12. Ground settlement-time-filling height change curves

Fig. 12 shows that the accumulative settlement value is low when the buried depth is high. Settlement is mainly concentrated in the reinforced area. The accumulative settlement values of MS-1, MS-2, MS-4, MS-5, and MS-7 are 11.2, 7.6, 6.5, 4.08, and 2.36 mm, respectively. The accumulative settlement of the subsoil in the short pile-reinforced area is 7.6 mm, which accounts for only 13.82% of the total settlement (55 mm) of the composite foundation. This result indicates the good reinforced control effect of the CFG short pile-net composite foundation in the gravel soil area.

##### 4.4.3 Analysis of the Lateral Displacement Test Results of the Foundation

Fig. 13 shows the lateral displacement change curves of the foundation with time. The figure indicates that the lateral displacement of the foundation increases with time (filling height) and is distributed in a bow shape along the depth direction. The main deformation area is located within 10 m below the surface, which accounts for over 75% of the total deformation. The lateral displacement curves of the foundation exhibit an inflection near the end of the piles in the reinforced area. This result occurs mainly because the high rigidity of the piles exhibits a certain constraint on the lateral displacement of the soil.

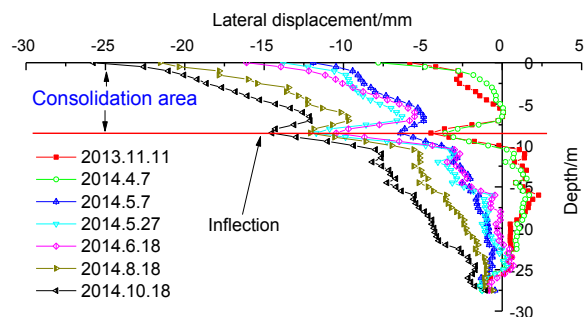


Fig.13. Lateral displacement change curves of the foundation with the time

Yu et al. [13] conducted a field test in the soft soil area at Chaoshan Station. The lateral displacements of the foundations in the selected test section reaches 30 mm to 45 mm and even up to 60 mm for individuals, which is 1.5 to 2 times higher than those of gravel clay (low to moderate compressible soil) foundations of the test section in the current study, which verifies the feasibility of the short pile reinforcement measure from the side.

##### 4.4.4 Foundation settlement law prediction

The main control objective of foundation treatment on high-speed railways is to reduce post-construction settlement.

Thus, predicting the post-construction settlement based on field test data is important in engineering applications. Fig. 14 shows the post-construction settlements of the foundation center predicted by the exponential curve method [5], hyperbola method [7], Hushino method [14], neural network method [12], and Asaoka method [16] based on the filed measured data.

Fig. 14 shows that the predicted data by the hyperbola method are consistent with the measured data. The accumulative settlement in 2000 days predicted by this method is 62 mm, and this outcome mainly occurs within 800 days. Thus, the accumulative settlement difference of the foundation fill during the static period of 400 days to 800 days is only 7 mm, which verifies that the overall reinforcement control effect of the gravel clay foundation after the construction period is effective after being treated with the short pile-net composite foundation.

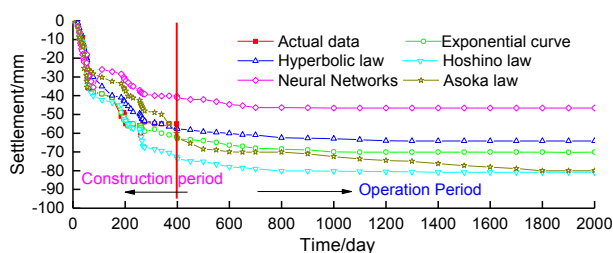


Fig.14. Settlement prediction change curves with the time

## 5. Conclusions

To investigate the behavior of a pile-net composite foundation, the short pile-net composite foundation on the Ganzhou-Longyan High-speed Railway was selected as an example to study the stress transmission law of the short pile-net composite foundation and the foundation settlement characteristics by conducting a field test with theoretical

analysis and analytic calculation as the bases. The conclusions drawn are as follows:

- (1) During the final stable phase, the pile-soil strain ratio is 4.0 and the pile-soil load sharing ratio is close to 50%. The pore water pressure at the end of the pile changes substantially, which verifies that the short piles can effectively transmit the increment of the additional stress of the upper load to the substratum from the side.
- (2) During the beginning of filling, the surface settlement rate is the largest at 0.63 mm/d. The accumulative settlement value reaches 38 mm, which accounts for 69.09% of the total value. The final accumulative settlement is 55 mm. The accumulative settlement of the substratum is 7.6 mm, which accounts for 13.82% of the total value.
- (3) The data predicted by the hyperbolic method are consistent with the measured data. This method has predicted that the accumulative settlement is 62 mm in 2000 days and that it mainly occurs within 800 days. The accumulative settlement difference is only 7 mm.
- (4) The lateral displacement of the foundation along the depth exhibits a bow shape. The lateral displacement within 10 m below the surface accounts for 75%, with the largest lateral displacement of 25 mm. The lateral deformation of the gravel clay foundation with low to moderate compressibility, which is approximately 60%, is lower than that of the soft soil foundation with high compressibility.

The behavior of the short pile-net composite foundation is studied based on the field-measured data to draw useful conclusions. However, future works should perform the following: conduct a comparative study of the behaviors of a long pile-net composite foundation, and a short pile-net composite foundation, among others.

## Acknowledgements

The study was supported by National Natural Science Foundation (Grant No. 51078358) and High-speed rail joint fund project (Grant No. U1134207).

## References

1. Han J, Gabr M A, "Numerical analysis of geosynthetic-reinforced and pile-supported earth platforms over soft soil", *Journal of Geotechnical and Geoenvironmental Engineering*, 128(1), 2002, pp. 44-53.
2. Zhao W, Yang G L, "Field experimental study on pile-soil stress ratio of pile-net composite foundation under embankment", *Hydrogeology & Engineering Geology*, 36(3), 2009, pp. 95-98.
3. Briancon L, Simon B, "Performance of pile-supported embankment over soft soil:full-scale experiment", *Journal of Geotechnical and Geoenvironmental Engineering*, 138(4), 2011, pp. 551-561.
4. Taechakumthorn C, Rowe R K, "Performance of a reinforced embankments on a sensitive Champlain clay deposit", *Canadian Geotechnical Journal*, 49(8), 2012, pp. 17-927.
5. Bourgeois E, DE B P, Hassen G, "Settlement analysis of piled-raft foundations by means of a multiphase model accounting for soil-pile interactions", *Computers and Geotechnics*, 46(11), 2012, pp. 26-38.
6. Zhang L, Zhao M, Hu Y, et al, "Semi-analytical solutions for geosynthetic-reinforced and pile-supported embankment", *Computers and Geotechnics*, 44(6), 2012, pp. 167-175.
7. Goit C S, Saitoh M, Mylonakis G, et al, "Model tests on horizontal pile-to-pile interaction incorporating local non-linearity and resonance effects", *Soil Dynamics and Earthquake Engineering*, 48(5), 2013, pp. 175-192.
8. Su D, Li J H, "Three-dimensional finite element study of a single pile response to multidirectional lateral loadings incorporating the simplified state-dependent dilatancy model", *Computers and Geotechnics*, 50(5), 2013, pp. 129-142.
9. Zhong R, Huang M, "Winkler model for dynamic response of composite caisson-piles foundations:Lateral response", *Soil Dynamics and Earthquake Engineering*, 55(12), 2013, pp. 182-194.
10. Zhang C, Jiang G, Liu X, et al, "Deformation performance of cement-fly ash-gravel pile-supported embankments over silty clay of medium compressibility:a case study", *Arabian Journal of Geosciences*, 8(7), 2014, pp. 1-13.
11. Zhang L, Luo Q, Liu X X, et al, "Cushion effect analysis of pile-net composite foundation based on field tests", *Journal of Southwest Jiaotong University*, 45(5), 2010, pp. 787-792.
12. Jiang G L, Zhang Z L, "Study on load transfer and settlement mechanisms in geosynthetics-reinforced floating-pile supported embankments over medium compressibility foundation", *Chengdu: Southwest Jiaotong University*, 2015, pp. 35-67.
13. Yu J J, Chen Q G, Li C H, et al, "Field test study of pile-net composite foundation on oversized deep soft soil", *Rock and Soil Mechanics*, 10(33), 2012, pp. 2881-2889.
14. Xu L R, Wang H G, Zuo S, et al, "Test study of performance of composite pile foundation of high-speed railway controlling settlement", *Rock and Soil Mechanics*, 33(9), 2012, pp. 2605-2612.
15. Gong X N, "Composite foundation theory and engineering application", *Beijing:China Building Industry Press*, 2002, pp. 180-232.

16. Chen H W, Xu L R., "Filed experiment of pile-soil stress ratio of pile-raft(net)composite foundation", *Hydrogeology & Engineering Geology*, 6(41), 2014, pp. 63-69.